Spectroscopic, Kinetic, and Electrochemical Characterization of Heterologously Expressed Wild-Type and Mutant Forms of Copper-Containing Nitrite Reductase from *Rhodobacter sphaeroides* 2.4.3[†]

Kenneth Olesen,[‡,§] Andrei Veselov,[∥] Yiwei Zhao,[∥] Yousheng Wang,[‡] Birgit Danner,[∥,⊥] Charles P. Scholes,[∥] and James P. Shapleigh*,[‡]

Department of Chemistry, Center for Biophysics and Biochemistry, University at Albany, SUNY, Albany, New York 12222, and Department of Microbiology, Wing Hall, Cornell University, Ithaca, New York 14853

Received July 2, 1997; Revised Manuscript Received February 3, 1998

ABSTRACT: We report the development of a high-yield heterologous expression system for the copper-containing nitrite reductase from a denitrifying variant of *Rhodobacter sphaeroides*. Typical yields of wild-type protein are 20 mg L^{-1}, which can be fully loaded with copper. Nitrite reductase contains an unusual blue-green Type 1 copper center with a redox/electron transfer function and a nearby Type 2 center where nitrite binds and is reduced to nitric oxide. The wild-type enzyme was characterized by: (1) its blue-green Type 1 optical spectrum; (2) its EPR spectrum showing rhombic character to its Type 1 center and nitrite perturbation to its Type 2 center; (3) its 247-mV Type 1 midpoint potential which is low relative to other Type 1 centers; and (4) its kinetics as measured by both steady-state and stopped-flow methods. The Type 2 copper reduction potential as monitored by EPR in the absence of nitrite was below 200 mV so that reduction of the Type 2 center by the Type 1 center in the absence of nitrite is not energetically favored. The mutation M182T in which the methionine ligand of Type 1 copper was changed to a threonine resulted in a blue rather than blue-green Type 1 center, a midpoint potential that increased by more than 100 mV above that of the wild-type Type 1 center, and a somewhat reduced nitrite reductase activity. The blue color and midpoint potential of M182T are reminiscent of plastocyanin, but the Type 1 cupric HOMO ground-state electronic *g* value and copper hyperfine properties of M182T (as well as cysteine and histidine ENDOR hyperfine properties; see next paper) were unchanged from those of the blue-green native Type 1 center. His^{287} is a residue in the Type 2 region whose imidazole ring was thought to hydrogen bond to the Type 2 axial ligand but not directly to Type 2 copper. The mutation H287E resulted in a 100-fold loss of enzyme activity and a Type 2 EPR spectrum (as well as ENDOR spectra; see next paper) which were no longer sensitive to the presence of nitrite.

Bacteria have the ability to utilize a wide range of terminal electron acceptors. For example, nitrate is used by both eubacteria and archea as an alternative electron acceptor when oxygen is limiting. One environmentally important form of nitrate respiration, referred to as denitrification, results in the conversion of fixed forms of nitrogen, such as nitrate or nitrite, to nitrogen gas. The defining reaction of denitrification, unique to the denitrification process and catalyzed by nitrite reductase (Nir),[1] is the one-electron reduction of nitrite to nitric oxide, the initial gaseous intermediate produced in this process. The nitric oxide produced by Nir is reduced to nitrous oxide by NO reductase (Nor), which is related to the heme-copper family of cytochrome *c* oxidases (*1*). The activity of NO reductase is required to prevent NO from accumulating to lethal concentrations. It has recently been shown that Nir activity is required for the expression of the genes encoding both Nir and Nor (*2*). The dependence of gene expression on Nir activity is a consequence of NO being the molecule that signals when conditions are suitable for nitrite reduction (*3*). It is not surprising that NO is used as a signal molecule by bacteria; the role of NO as a signal molecule in higher organisms is already well documented (*4*).

There are two types of denitrification-associated nitrite reductases, one of which contains copper and the other heme.

[†] These studies were partially supported by the NIH (GM-35103, C.P.S.) and the USDA (J.P.S.).

* To whom correspondence should be addressed: Phone: 607-255-8535. Fax: 607-255-3904. E-mail: jps2@cornell.edu.

[‡] Cornell University.

[§] Present address: Department of Biochemistry and Biophysics, Lundberg Institute, Göteborg University and Chalmers University of Technology, Medicinaregaten 9C, S-413 90, Göteborg, Sweden.

[∥] University at Albany.

[⊥] Present address: Department of Physics, Würzburg University, Am Hubland, 57074 Würzburg, Germany.

[1] Abbreviations and definitions: Nir, nitrite reductase; Nor, nitric oxide reductase; IPTG, isopropyl β-D thiogalacto pyranoside; ICP, inductively coupled plasma emission spectroscopy; MES, 2(N-morpholino) ethanesulfonic acid; WT, wild-type or native Nir; M182T, a mutant form of Nir where the Met^{182} ligand at the Type 1 center was mutated to threonine; H287E, a mutant form of Nir where the His^{287} residue near, but not liganding to the Type 2 center, was mutated to glutamic acid; TD, abbreviation for Nir depleted of Type 2 copper; cyt *c*, cytochrome *c*; cyt c^{2+}, ferrocytochrome *c*; ptp, peak-to-peak; G, gauss; kG, kilogauss; i.d., inside diameter; o.d., outside diameter; EPR, electron paramagnetic resonance; ENDOR, electron nuclear double resonance.

S0006-2960(97)01603-6 CCC: $15.00
Published on Web 04/04/1998

The three-dimensional structures of copper-containing Nir have been solved and reveal that Nir is a homotrimer with two copper atoms bound per monomer (*5*, *6*). One of these copper atoms is liganded by two His, one Cys, and one Met. Copper centers as found in plastocyanin (*7*) or azurin (*8*) with this set of ligands are referred to as Type 1 copper centers and are typically characterized by their blue color (intense absorption band near 600 nm). The copper Nir from *Achromobacter cycloclastes* (*9*), *Rhodobacter sphaeroides* f. sp. *denitrificans* (*10*) and *Alcaligenes faecalis* (*11*) and from the present protein are blue-green in color due to comparably intense absorption bands near 600 and 450 nm. The unusually short Met(S)−Cu bond, a longer Cys(S)−Cu bond distance, and altered bond angles are structural differences from more widely studied blue proteins that may contribute to the unusual spectroscopic properties of Type 1 copper in Nir. Spectroscopies that probe transitions to excited electronic states (*12*) have given evidence for electronic differences between Type 1 centers, and LaCroix et al. (*12*) combined spectroscopic investigations with density functional calculations to define what was called "the extremely 'perturbed' electronic structure of this site relative to that of the prototypical 'classic' site in plastocyanin". [Plastocyanin is prototypical and classical from the standpoint that its 3-dimensional structure was the first one reported for a blue protein (*7*).] The midpoint potentials of blue proteins range from 184 mV for stellacyanin (*13*) to 230−320 mV for azurins (*14*), 370 mV for plastocyanins (*15*), and 680 mV for rustacyanin (*16*). The midpoint potential for the wild-type blue-green Type 1 center in Nir (*17*) is near the lower end of the range at ∼250 mV. The other copper center in Nir is bound by three His residues and belongs to the Type 2 class of copper centers having larger $A_{||} - g_{||}$ values and much lower optical absorbance than Type 1. The Type 2 center has been shown to be the site of nitrite binding (*5*, *6*), while the Type 1 center is necessary for transfer of electrons from biochemical reductants such as pseudoazurin or ferrocytochrome to the Type 2 center (*18*, *19*). A schematic of the environs of these centers after ref 6 is provided in Figure 1 of the accompanying paper; Type 1 and Type 2 copper are 12.5 Å apart.

We have recently characterized the gene encoding the copper-containing Nir from *R. sphaeroides* 2.4.3. Alignment of the amino acid sequences of Nir from 2.4.3 with other copper-containing Nir reveals a high degree of amino acid identity between the sequences (*2*). In fact, the *R. sphaeroides* Nir is one of the more divergent sequences, but it still has at least 60% identity with the other sequences. This suggests there are significant structural constraints that result in Nir being intolerant of changes in the primary sequence. One such constraint may be that which tunes the Type 1 midpoint potential and concomitantly alters its spectroscopic properties. The axial Met^{182} is a prime candidate for altering Type 1 properties (*12*). The nitrite-binding process may also be constrained by near but nonliganding neighbors of the Type 2 center. His^{287} is one such neighbor whose interaction with nitrite is suggested by X-ray data (*6*). As an extension of our work on NO metabolism in *R. sphaeroides* 2.4.3, we developed rapid, high-yield expression and purification protocols for *R. sphaeroides* 2.4.3 Nir. With the realization that NO plays a role as both a respiratory substrate and a signal molecule in 2.4.3, we wanted to undertake a more detailed study of the enzyme responsible for NO production. In this paper we describe spectroscopic, kinetic, and electrochemical analyses of heterologously expressed wild-type Nir. This significantly extends the previous work on *R. sphaeroides* Nir and provides information necessary for a comparative analysis of wild-type and site-directed mutant forms of Nir generated to probe structure−function relationships. A characterization of two mutants, M182T and H287E, is also presented here. These two mutations were chosen for study because each is in a position to alter electronic structure and enzyme function but in ways more subtle than simple elimination of a copper center. In this paper a direct functional demonstration is provided of how Nir structure influences redox behavior and enzyme turnover, and in the next paper an ENDOR spectroscopic demonstration is provided of how the Nir structure concomitantly influences the intimate electronic distribution at the metal centers.

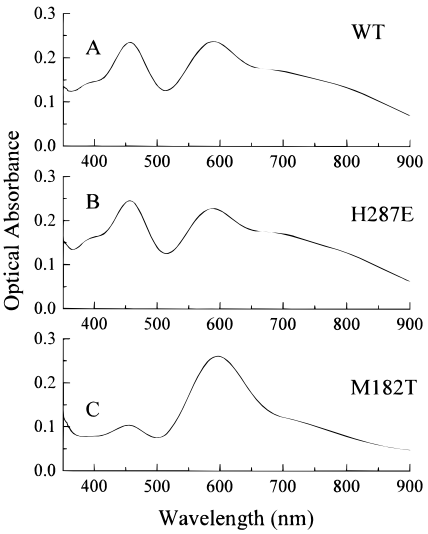

FIGURE 1: UV−vis spectra of WT Nir (A), the H287E mutant (B), and the M182T mutant (C). The concentrations of Type 1 copper were approximately 0.1 mM. The buffer was 0.05 M, pH 7.1 potassium phosphate.

METHODS AND MATERIALS

Materials

Construction of Vectors for Heterologous Expression. Initial development of the Nir expression system was done by inserting *nirK*, which encodes Nir, into pMAL-C2; the resultant vector, pMAL-C2nirK, provided a recombinant Nir fusion protein (MalENir) having a maltose-binding domain. However, each ∼37-kDa Nir subunit of MalE-Nir was fused to a ∼43-kDa MalE maltose-binding fragment, and it was considered important to develop a nonfusion expression system lacking such a large extraneous section of polypeptide. The detailed development of pMAL-C2nirK is outlined in the Supporting Information to this paper.

A heterologous expression system independent of the maltose-binding fragment was developed using the vector pET-17b (Novagen). To clone *nirK* into pET-17b, a 0.8-kb *Eco*RI−*Xho*I fragment from pMAL-C2nirK was ligated into pET-17b restricted with *Eco*RI and *Xho*I. This clone was then digested with *Sph*I and *Xho*I, and a *Sph*I−*SalI* fragment from pMAL-C2nirK was inserted to reassemble an intact *nirK*. The expected size of the product of the gene fusion

in the pET clone is 41 kDa. Since the recombinant Nir is expressed cytoplasmically, it is not processed during export and thus leaves 36 residues at the N terminus that would normally be removed. The downstream 336 residues are identical to those of WT Nir.

Purification of Nir. *Escherichia coli* BL21 was used as a host for pET17b-*nirK*. Cells were grown at 37 °C with agitation in Luria broth (*20*) supplemented with 600 μM copper to an A_{600} of 0.5, and expression of the *nirK* was induced by addition of 85 mg L^{-1} IPTG. After this addition, the cells were allowed to grow for 2 h. Cells were then harvested by centrifugation and resuspended in 40 mL of 50 mM phosphate buffer, pH 7.2. Typically, 2 L of cells were used for each purification. Cells were broken by passage through a French press, and cell debris was removed by centrifugation at 12000*g* for 15 min. The supernatant was transferred to 15-mL polypropylene tubes and placed in a 70 °C water bath for 10 min. Precipitated protein was removed by centrifugation at 27000*g* for 30 min. One milliliter of 0.1 M $CuCl_2$ was added dropwise with stirring to the supernatant since nonfusion Nir required additional *in vitro* inorganic copper for its reconstitution.[2] [The Nir−maltose fusion protein (MalENir) incorporated sufficient copper in vivo if copper was added to the growth medium.] The resultant extract was loaded onto a Q-Sepharose (Sigma) fast-flow anion exchanger, column size 25 × 60 mm. The extract was washed with 20−30 column volumes of resuspension buffer, then washed with 5−10 volumes of phosphate buffer that was 300 mM in NaCl, and finally eluted by the addition of phosphate buffer that was 400 mM in NaCl.[3] The purified protein was desalted by passage over Bio-Gel P-6 DG 130 and then dialyzed overnight versus two changes of 0.05 M pH 7.2 phosphate buffer. Typical yields of the protein were 20 mg L^{-1}. The enzyme was concentrated by an Amicon concentrator and stored at −80 °C. Size analysis of the purified protein by gel filtration was carried out using a Sephacryl S-200 HR FPLC column (Pharmacia), calibrated by ovalbumin (47 kDa), albumin (67 kDa), alcohol dehydrogenase (150 kDa), and β-amylase (200 kDa).

To make Type 2 depleted wild-type Nir (TD-WT), 2−3 mL of 100 μM enzyme was dialyzed at 4 °C for 18 h versus 1 L of nitrogen-flushed 50 mM acetate buffer (pH 5.2) for TD-WT that contained 2 mM dimethylglyoxime, 1 mM EDTA, and 5 mM ferrocyanide. Making Type 2 depleted mutant enzyme presented greater difficulty because the mutant enzymes appeared less resistant to simultaneous removal of both Type 1 and Type 2 copper. To make TD-M182T and TD-H287E, this dialysis was performed at pH 5.8 for less than 4 h with frequent monitoring for Type 1 color loss. Next, the enzyme was dialyzed overnight versus 50 mM phosphate buffer pH 7.2. Type 2 depleted enzyme was used for estimating the Type 1 copper optical extinction coefficients.

Methods

Spectroscopic Methods. Optical spectra were recorded with a Shimadzu dual beam spectrophotometer (slit width = 1.0) or a Beckman DU 640 spectrophotometer. The Shimadzu was also used in a single-beam mode to collect redox titration data. Steady-state enzymatic turnover information from oxidation of ferrocytochrome *c* was monitored with a Perkin-Elmer 552. X-band EPR was carried out with an ER-200 IBM Bruker X-band spectrometer equipped with standard rectangular TE_{102} X-band EPR cavity and either an APD Cryogenics LTR-3 Helitran system (Allentown, PA) or a Wilmad WD 816 Dewar flask. EPR data were collected in the Zenith 386 computer using the EW Software routines (Scientific Software Sales). Copper content was measured by inductively coupled plasma (ICP) emission spectroscopy and by the 2,2′ biquinoline assay (*21*).

Activity Measurements. Measurements were performed with both limited turnover (stopped-flow) and steady-state methods. For the *R. sphaeroides* Nir under study, the precise electron donor to Type 1 copper is unknown but has been suggested to be a *c* type cytochrome (*22*). Eukaryotic ferrocytochrome *c* was chosen as a reductant because it is commercially available and has previously been demonstrated to be an effective electron donor in Nir studies (*23*). We found that yeast cytochrome *c* (*Saccharomyces cerevisiae* cytochrome *c*, 99% purity, Sigma) provided more rapid turnover than horse cytochrome *c* (Type VI, Sigma).[4] The reduction potential of ferrocytochrome (cyt c^{2+}) is 285−290 mV (*24*) and is comparable to that of the Type 1 center. The cyt *c* was reduced with ascorbate and the ascorbate removed by A-25 DEAE Sephadex resin (Pharmacia). Stopped-flow measurements of Nir activity under anaerobic, argon-flushed conditions were done by rapid mixing of cyt c^{2+} and nitrite with Nir. Oxidation of cyt c^{2+} was monitored in the Aminco-Morrow stopped-flow attachment coupled to a retrofitted DW-2 UV−vis spectrophotometer [the original by SLM Instruments, Urbana, IL, with retrofit by On Line Instrument Systems (OLIS), Inc., Jefferson, GA]. Kinetic data collection software and kinetic fitting software were provided by OLIS. Complementary steady-state activity measurements using nanomolar concentrations of enzyme and varying concentrations of nitrite and cyt c^{2+} at the micromolar range and above were performed (*23*). This work was carried out at pH 6.2 in 50 mM MES buffer so that turnover rates might be compared with the results of refs 23 and 25. The initial rate of cyt c^{2+} reduction, which only occurred in the presence of nitrite when Nir was present, was monitored at 550 nm. The number of reducing equivalents consumed was determined by the relation $\Delta\epsilon_{(Red-Ox)550} = 2.1 \times 10^4\ M^{-1}\ cm^{-1}$ (*26*).

Reduction Potentials. Potentials were measured with an Ingold-Metler/Toledo combined redox electrode (Pt4805-S7)

[2] A different method of additional copper incorporation was to add a 30-fold molar excess of $CuCl_2$ to the purified Nir and incubate, with stirring, under nitrogen gas for 96 h at 4 °C. After incubation the protein solution was dialyzed against 50 mM phosphate buffer with 1 mM EDTA for 12 h. Then the protein was dialyzed against phosphate buffer for 24 h with three changes of dialysis buffer.

[3] An additional FPLC Q-sepharose purification step was also performed upon one preparation of each of the WT and mutant enzymes. The protein was eluted with a 300−600 mM NaCl gradient. This additional procedure led to an enzyme with unchanged spectroscopic properties and an undiminished Cu/protein ratio.

[4] For the purpose of comparing activities of *Rhodobacter sphaeroides* Nir and its mutants, the yeast cytochrome served well. The cyt c^{2+} turnover number is expectedly smaller than the turnover number of *Alcaligenes faecalis* pseudoazurin reductant as brought on by *A. faecalis* Nir (*18*) because the *A. faecalis* pseudoazurin was undoubtedly the natural substrate for *A. faecalis* Nir, whereas yeast cytochrome *c* is only an approximate substrate of *R. sphaeroides* Nir.

after methods of ref 13. Ascorbate and ferricyanide were the reductants and oxidants, respectively, and *N*,*N*,*N*′,*N*′-tetramethyl-*p*-phenylenediamine and 2,6-dichlorophenol-indo-phenol (Sigma) in micromolar concentrations were used as redox mediators. These measurements were performed under an argon atmosphere. The optical absorbance at 585 nm due to oxidized Type 1 copper was monitored spectrophotometrically, and entire optical traces from 700 to 400 nm were taken at each potential with a wait of at least 15 min to achieve redox equilibrium between additions of oxidant or reductant. For EPR measurements related to redox potential measurements, samples were withdrawn by gastight syringe from the vessel containing the redox electrode, loaded into argon-flushed EPR tubes, and rapidly frozen.

RESULTS

Preparative Results. Induction of *nirK* expression by IPTG led to the overexpression of a protein close to the predicted size of the recombinant Nir monomer. Centrifugation of cell extracts indicated that the protein was soluble with little production of insoluble aggregates. Purification of Nir was carried out using a variation of the protocol for purification of Nir from *R. sphaeroides* f. sp. *denitrificans*, which takes advantage of the heat resistance of Nir (*10*). The purification procedure is rapid, and it can be completed in 1 day. Typical yields of the recombinant Nir using the modified procedure were ~20 mg L^{-1} with WT protein and slightly less for the mutants, yields significantly higher than Nir heterologously purified from periplasmic-based expression systems (*18*). Analysis by gel filtration yielded a single high molecular mass peak of 140 ± 15 kDa, indicating that the WT enzyme and both mutants are almost all trimers. SDS−PAGE analysis provided a single band from the WT enzyme and both mutants, indicating a level of purity equivalent to that of Nir purified from *R. sphaeroides* f. sp. *denitrificans* (*10*).

Protein purified using this procedure contained no copper, even though the cells were grown in a medium amended with copper, but copper could be reincorporated by addition to the partially purified apoprotein. It is unlikely that the lack of copper incorporation was a direct consequence of cytoplasmic expression since a MalE-Nir fusion protein (see Supporting Information) contained copper if purified in cells grown in the presence of copper. It is unclear why copper is not incorporated during expression in the pET-based expression system.

Copper Content. The total copper content was determined by ICP and 2,2′ biquinoline analysis of the copper content (*21*). Based on the Bradford assay (*28*) of the protein content, the WT enzyme contained 2.0 ± 0.3 Cu per 41-kDa monomer subunit. The uncertainty in the copper content reflects the variation in copper content between preparations and also the variation between the ICP and biquinoline methods. The Type 1:Type 2 ratio for WT enzyme, as determined from the Type 1 optical spectrum and from the difference between overall copper and Type 1 copper, was 1:1. The mutant enzymes contained less overall copper per subunit than WT; M182T contained 1.2 ± 0.2 Cu per 41-kDa monomer subunit, and H287E contained 1.0 ± 0.2 Cu per 41-kDa subunit. As has been noted for other mutants of heterologously expressed copper-containing proteins, the copper incorporation was reduced [albeit nowhere near as significantly as the 20% copper incorporation in azurin mutants (*29*)]. However, our mutagenesis did not result in the total loss of a particular copper center; the Type 1 center is obviously present in M182T and the Type 2 center is obviously present in H287E, as shown by EPR of both centers and the optical spectrum of the Type 1 center in M182T.

Table 1. Optical Properties

sample	λ (nm)	$R_{(\lambda/590)}$[a]
wild-type	390 ± 4 (pk)	0.60 ± 0.05
	457 ± 2 (pk)	1.00 ± 0.05
	589 ± 2 (pk)	1.00
	700 ± 20 (sh)	0.72 ± 0.05
	810 ± 20 (sh)	0.53 ± 0.05
H287E	393 ± 4 (pk)	0.60 ± 0.05
	456 ± 2 (pk)	1.10 ± 0.05
	587 ± 2 (pk)	1.00
	710 ± 20 (sh)	0.73 ± 0.05
	810 ± 20 (sh)	0.53 ± 0.05
M182T	452 ± 2 (pk)	0.40 ± 0.05
	596 ± 2 (pk)	1.00
	740 ± 20 (sh)	0.40 ± 0.05

[a] $R_{(\lambda/590)}$ is the ratio of the absorption peak at wavelength λ to the absorption peak at 590 nm.

Optical Spectra. The copper Nir from *A. cycloclastes* (*9*, *17*, *25*), *R. sphaeroides* f. sp. *denitrificans* (*10*), and *A. faecalis* (*11*) and from the protein described in this paper is blue-green in color due to an intense absorption near 450 nm in addition to the more generally expected absorption near 600. Although exact ratios of ~450 to ~590 absorbances vary between Nir from various sources, the 450-nm absorbance was much larger compared to the 590-nm absorbance than in blue type cupredoxins. Optical properties are listed in Table 1. The 2.4.3 Nir in its WT form had peak maxima at 589 and 457 nm (Figure 1A), and the ratio of these peak absorbances was approximately unity. In addition we noted in the 700−900 region broad features at approximately 700 and 810 nm; such near-IR features of cupredoxins may have d−d character (*30*). We show also the corresponding optical spectra of H287E (Figure 1B), whose peak frequencies and peak ratios are virtually identical to those of WT Nir. The M182T mutant, which was blue, had an optical absorbance (Figure 2 C) changed toward that of a more typical blue Type 1 copper protein. Its major absorbance occurred at a slightly higher wavelength (596 nm) than with WT or H287E; the feature at 452 nm was only 40% as intense as the peak at 596 nm; there appeared to be only one broad feature near 740 nm in the near-IR region. Regardless of the absolute extinction coefficients (below), the ratio of peak intensities directly obtained from the enzyme without depletion of Type 2 simply and accurately showed the differences between the optical spectra of blue-green WT and H287E on one hand and the blue M182T mutant form on the other hand. The ratio of 450- to 600-nm absorbances for plastocyanin and azurin is ~0.06 (*31*).

To determine absolute values of optical extinction coefficients for Type 1 copper rather than ratios of peak absorbances, we determined separately the amount of Type 1 (not total) copper with Type 2 depleted (TD) enzyme from which the optical absorbance had also been measured.[5] The spectra of the TD-WT, TD-H287E, and TD-M182T forms

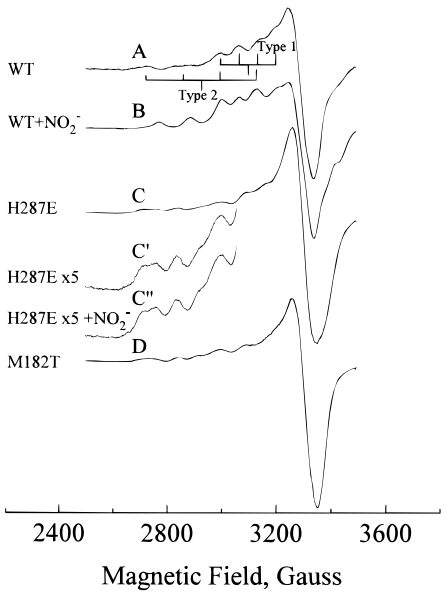

FIGURE 2: X-band EPR spectra of WT and mutant Nir. Spectra were obtained at $T = 77$ K, $\nu_e = 9.42$ GHz, 100-kHz modulation = 10 G ptp, 2-mw power, pH 7.1, 0.05 M potassium phosphate buffer. Enzymes were approximately 0.5 mM in total copper. (A) EPR spectrum of WT Nir. (B) WT Nir in the presence of 6 mM nitrite. (C) EPR spectrum of H287E; the insets below this spectrum show the unchanged spectra at a 4-fold higher gain from the Type 2 copper in the absence (C′) and in the presence (C″) of 6 mM nitrite. (D) EPR spectrum of M182T.

are given in Figure S-1 in the Supporting Information. Extinction coefficients for the 589- and 457-nm peaks of WT Type 1 copper, as obtained from TD-WT enzyme, were $(2.3 \pm 0.3) \times 10^3$ M^{-1} cm^{-1}, and the WT extinction coefficients at other wavelengths may be determined from this extinction coefficient and from the ratio of peak intensities in Table 1. (The uncertainty in the extinction coefficient reflects the variation in measured Type 1 copper content between preparations.) The molar extinction coefficient for WT enzyme at 280 nm was 4.3×10^4 M^{-1} cm^{-1} per subunit, as determined by the assay of Gill and von Hippel (*32*). The absolute extinction coefficients for Type 1 copper of the H287E and M182T mutants had a larger uncertainty due to the difficulty of making them Type 2 depleted. The extinction coefficients as measured from TD-M182T were $(1.7 \pm 0.5) \times 10^3$ M^{-1} cm^{-1} for the intense peak at 596 nm and $(0.7 \pm 0.2) \times 10^3$ M^{-1} cm^{-1} for the weaker peak at 452 nm. Although the spectrum of H287E including the ratio of peak absorbances (Figure 1B) was markedly similar to that of the WT enzyme and although we would expect the extinction coefficients of its Type 1 copper therefore to be the same as for WT enzyme, the absolute extinction coefficients of Type 1 copper in H287E, based on copper determination and optical absorbance of TD-H287E, were about one-half of those of the WT enzyme.

EPR Spectroscopy. Figure 2 shows EPR spectra from both the Type 1 and Type 2 copper of Nir in its WT and mutant forms. EPR signals of WT enzyme are similar to those reported in refs 17, 18, and 25 with similar relative intensities of Type 1 and Type 2 features. The Type 2 features occurred at X-band without obstruction from Type 1 features at g values greater than ~2.21 and magnetic fields less than 2.9 kG. In the absence of nitrite (Figure 2A) the lower-field Type 2 features that have $M_I = {}^3/_2$, ${}^1/_2$ provided evidence of $A_z = 125 \pm 35$ G ($1.36 \pm 0.38 \times 10^{-2}$ cm^{-1}) and $g_z = 2.34 \pm 0.03$. In the presence of nitrite the Type 2 features sharpened and the g value and hyperfine couplings slightly diminished to $A_z = 112 \pm 12$ G ($1.19 \pm 0.13 \times 10^{-2}$ cm^{-1}) and $g_z = 2.30 \pm 0.01$ (Figure 2B); a changed Type 2 EPR signal in the presence of nitrite had previously been noted (*25*, *33*). For the H287E mutant (Figure 2C), the Type 2 features still remained despite the mutation near the Type 2 center, but these Type 2 features of H287E did not respond to the presence of nitrite as shown in the 5-fold higher gain insets comparing the H287E Type 2 features in the absence of nitrite (Figure 2C′) and the presence of nitrite (Figure 2C″). There was broadening and possible doubling of the lowest-field $M_I = {}^3/_2$ feature of the Type 2 copper of H287E. Figure 2D shows that the Type 2 features of M182T occurred in the same field region as those of WT, but there was more broadening and possible doubling of these features as well; the Type 2 features of a mutant form of *A. faecalis* Nir having a mutation at the Type 1 center were similarly perturbed (*18*). M182T showed the nitrite-induced change to its Type 2 features.

Type 1 A_z and g_z features, though somewhat overlapped with Type 2 $M_I = -{}^1/_2$ and $-{}^3/_2$ features, were evident. Type 1 features were naturally best resolved in the Type 2 depleted samples; the EPR spectra of Type 2 depleted WT and Type 2 depleted M182T are respectively compared in spectra A and B in Figure 3; with the exception of slightly greater breadth to the features of TD-M182T, the spectra are identical. Type 1 copper of WT Nir has been suggested to have a distorted copper site as shown by rhombic distortion in its $g_\perp$ region (*12*), and accordingly, second derivative ($d^2\chi''/dH^2$) presentations of spectra C (TD-WT) and D (TD-M182T) in Figure 3 showed low-field rhombic features. Thus the EPR parameters for Type 1 copper of both TD-WT and TD-M182T are the following: $A_z = 67 \pm 5$ G ($0.68 \pm 0.5 \times 10^{-2}$ cm^{-1}), $A_x = 50 \pm 10$ G ($0.48 \pm 0.10 \times 10^{-2}$ cm^{-1}); $g_z = 2.19 \pm 0.002$, $g_x = 2.02 \pm 0.006$ (the minimal g value associated with A_x) and $g_y = 2.06 \pm 0.002$ (g value at the high-field derivative crossing). The TD-WT and TD-M182T have markedly similar EPR spectra and rhombicities even though TD-WT has a blue-green center and TD-M182T is blue. In frozen solution M182T and TD-M182T *retained* their blue color.

Limited Turnover and Steady-State Activity Measurements. Optical monitoring of the enzyme-dependent consumption of cyt c^{2+} in stopped-flow experiments provided a straightforward way to assess the activity of the recombinant Nir and to assess the effects of the two mutations. For these measurements the concentrations of enzyme, cytochrome, and nitrite after mixing were 2.5, 10, and 50 μM, respectively. The enzyme concentration in all cases was explicitly normalized to the same amount of total copper for all samples and approximately to the same concentration of Type 1 copper. Figure 4 compares the spectrophotometrically monitored consumption of cyt c^{2+} occurring within 400 ms after mixing, as brought on by the WT, the M182T, and the

[5] In principle the EPR integration method of Aasa and Vänngård (*27*) could be used to determine separate Type 1 and Type 2 copper percentages, but we found that the EPR baseline uncertainty would propagate into ~2-fold variation in the ratio of Type 2 to Type 1 copper from this method.

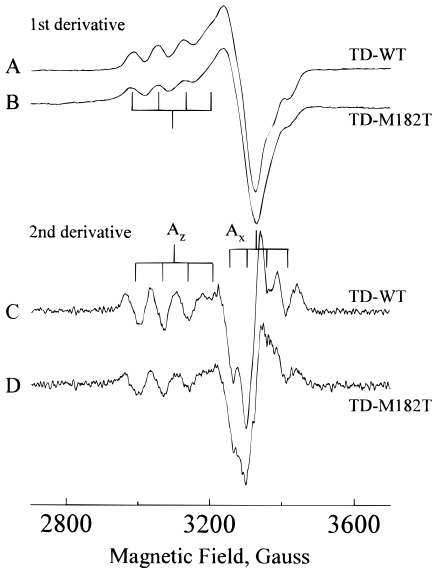

FIGURE 3: These spectra show first the absorption derivative ($d\chi''/dH$) EPR spectra of (A) the TD-WT enzyme and of (B) TD-M182T. The experimental conditions were the same as those for Figure 2. Spectra C and D, respectively, show the second derivative ($d^2\chi''/dH^2$) spectra of the TD-WT enzyme and TD-M182T with the purpose of showing the rhombic character of hyperfine coupling (A_x, g_x).

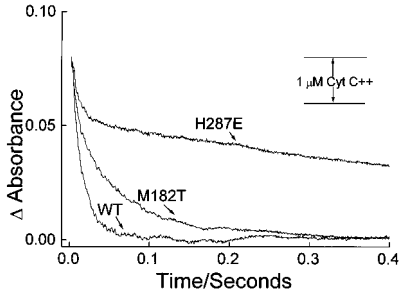

FIGURE 4: Rapid cyt c^{2+} consumption monitored by stopped-flow kinetics with the purpose of showing the different kinetics of cyt c^{2+} oxidation monitored at 550 nm, as brought on by WT, by M182T, and by H287E forms of Nir. Enzyme that was at ~2.5 μM concentration in Type 1 copper and 5 μM in total copper was reacted with a 4-fold molar excess of cyt c^{2+} and a 25-fold molar excess of nitrite in anaerobic pH 6.2, 0.05 M MES buffer. $T = 22$ °C.

H287E enzymes, respectively. Cyt c^{2+} consumption occurred for WT Nir within <50 ms of mixing and for M182T within ~100 ms of mixing. The amount of cyt c^{2+} consumed here was greater than the amount of Type 1 copper available, and other than for the initial very fast burst, turnover required nitrite. For H287E the cyt c^{2+} consumption following the burst extended in time well beyond 400 ms. The increasing rate of enzyme activity in the order H287E, M182T, and WT is empirically obvious in Figure 4. Analysis of the kinetic data suggested biphasic kinetics where the fast burst, accounting for ~1.5 μM cyt c^{2+}, occurred with a rate of ~100 s^{-1} for WT, M182T, and H287E. The burst was followed by a second slower phase whose rate was ~50 s^{-1} for WT enzyme, ~20 s^{-1} for M182T, and ~1 s^{-1} for H287E; for WT, M182T, and H287E the ratio of these rates was 1:0.4:0.02.

In the course of the complementary steady-state turnover experiments, nitrite concentrations were varied from 1 to 500 μM, and the initial rates of cyt c^{2+} consumption brought on by nanomolar concentrations of Nir were determined. For the WT enzyme a turnover number of 1600 ± 700 (mol of cyt $c^{2+}$$min^{-1}$/mol of Type 1 copper) was estimated from the maximum rate of cyt c^{2+} consumption and the concentration of Type 1 copper. See Supporting Information, Figure S-2, for double-reciprocal plots of rates of cyt c^{2+} consumption versus nitrite concentration, from which the turnover number and a K_m value were estimated.[6] On the basis of available milligrams of WT Nir protein, as determined by the Bradford assay (*28*), the maximum rate of cyt c^{2+} consumption translated to ~35 μM c^{2+}/mg WT protein min^{-1}, an activity comparable with that reported by the similar cytochrome-based Nir assays (*23*, *25*).[4] When an initial concentration of 250 μM cyt c^{2+} was used, the maximum rate of cyt c^{2+} consumption by WT Nir in the presence of 100 μM nitrite was the same as when 20 μM cyt c^{2+} was used. Based on the Type 1 copper concentration (determined from $\epsilon_{596} = 1.7 \times 10^3$ M^{-1} cm^{-1} for M182T and $\epsilon_{589} = 2.3 \times 10^3$ M^{-1} cm^{-1} for H287E), the turnover number of cyt c^{2+} consumption for the M182T was 150 ± 50 (mol of cyt $c^{2+}$$min^{-1}$/mol of Type 1 copper), and for the H287E it was 5 ± 3 (mol of cyt c^{2+} min^{-1}/mol of Type 1 copper). The K_m value for WT was 14 ± 7 μM and for the H287E and M182T ~4 μM.[6] The differences in the maximum rates of cyt c^{2+} consumption between WT Nir and the mutants qualitatively mirrored the differences in activity measured by the limited-turnover, stopped-flow measurements above; for the WT, M182T, and H287E the ratio of turnover numbers was 1:0.1:0.003.

Midpoint Potential. There has been only limited characterization of the midpoint potentials of copper-containing Nir (*17*). It is critical to determine the relative potentials of the metal centers to develop a model of Nir function. In particular it is important to understand the relationship between redox behavior and the electron-transfer function of the Type 1 center. Redox titrations for Type 1 copper are shown in Figure 5 as Nernst plots, where Log_{10}([Ox]/[Red]) was plotted versus the electrode potential, *E*, for WT protein and the H287E and M182T mutants. The ratio of oxidized to reduced Type 1 copper, {[Ox]/[Red]}, was obtained from the ratio of absorbances, $(A_{585} - A^r)/(A^o - A_{585})$. A^o was the absorbance at 585 nm when the Type 1 center was completely oxidized, and A^r was the absorbance at 585 nm when the Type 1 center was completely reduced. The midpoint reduction potential for the WT and H287E was 247 ± 15 mV, whereas the midpoint reduction potential for the Type 1 copper of the blue M182T mutant was 354 ± 18 mV.[7] The reduction potential of M182T is ≥100 mV higher

[6] As determined from the double-reciprocal plot in the Supporting Information, the K_m (nitrite) of WT Nir, M182T, and H287E were respectively 14 ± 7, 3.5 ± 2, and 4 ± 2 μM.

[7] Our major goal for these redox titrations was to find evidence for the difference in midpoint reduction potentials between the WT and mutant forms, and we have unequivocally done this. We note that for M182T the slope of the redox titration curve was 84 mV/decade rather than the 60 mV/decade slope expected for an $n = 1$ Nernstian titration. Although such a deviation in slope could represent the complication of intersite interactions in this multimetal, multisubunit protein, we point out that comparable deviations in slope have been reported for mutants of the monosubunit Type 1 protein, azurin (*34*). For the titration of ref 34 there was permanent loss of optical absorption correlated with the loss of copper; in our titration the deviation in slope was still evident over the course of 1.5-h titrations where no permanent loss of optical absorption occurred. A 4.5-h titration did lead to 20% permanent loss of absorption as might occur if Type 1 copper were lost.

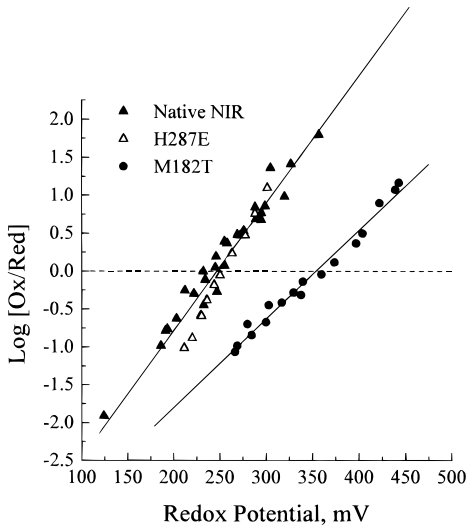

FIGURE 5: These traces show redox titrations in the form of Nernst plots for Type 1 copper belonging to WT (solid triangles), H287E (open triangles), and M182T (solid circles). The midpoint potential for WT and H287E was 247 ± 15 mV with a slope of 59 mV/decade. For M182T the midpoint potential was 354 ± 18 mV with a slope of 84 mV/decade.

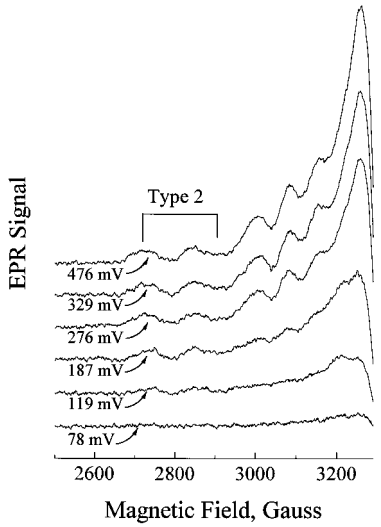

FIGURE 6: This figure shows a compendium of WT Nir X-band EPR spectra taken from enzyme equilibrated at the electrode potentials (SHE) indicated on the spectra. The purpose of this figure is to show that the characteristic Type 2 EPR features in the low-field $A_{||} - g_{||}$ region were not abolished until the potential was below 200 mV.

than that of the WT enzyme and is close to the potential found for plastocyanin (*15*). The comparison of the midpoint potentials of the Type 1 copper center in WT and M182T demonstrates that the redox potential can be significantly modulated by its axial ligand.

In the course of redox titrations, the optically invisible but EPR-detectable Type 2 features of WT Nir were monitored, and Type 2 features persisted at potentials below 200 mV. The compendium of resultant Type 2 EPR spectra (Figure 6), obtained over a range of electrode potentials, enabled us to put an upper limit of 200 mV on the midpoint potential where half of the Type 2 EPR signal had been reductively eliminated. Two-hundred millivolts is a potential definitely below that of the WT Type 1 center. Other Type 2 copper systems have reduction potentials less than 200 mV (see, e.g., ref *35*). A reduction potential of the Type 2 center was estimated at 250 mV, but this estimate was obtained indirectly in the course of flash photolysis kinetic studies, not equilibrium redox studies (*17*).

DISCUSSION

Details of Preparation and Molecular Biology. The gene designated *nirK*, encoding the Nir, in the denitrifier *R. sphaeroides* 2.4.3 has recently been cloned and sequenced (*2*). Copper-containing Nir has not been shown to require ancillary proteins for assembly, and the Nir apoprotein can be reconstituted by incubation with copper (*25*). To maximize the production of Nir, our protocol was developed for heterologous expression in *E. coli.* Besides increasing expression because of copy number, the expressed protein was engineered so it remained cytoplasmic. This made it possible to overexpress Nir in the cytoplasm of *E. coli* and then to purify and reconstitute it. Export to the periplasm, the normal location of the WT enzyme, gives lower yield (*18*). A preliminary method involving a maltose-binding protein fusion (MalENir), which has been adapted as a component of a nitrite biosensor (*36*), gave high yields (see Supporting Information). However, because of the potential for alteration of the protein structure by the maltose-binding fragment, for the present work a form of Nir with only a small non-WT N-terminal sequence was expressed and purified. The present method of overexpression provides considerably larger quantities of pure protein needed for spectroscopy (e.g., the subsequent ENDOR study), electrochemistry (especially as monitored by EPR), and limited turnover kinetic studies required for probing the enzyme mechanism.

Wild-Type Enzyme. The optical and EPR properties of the WT enzyme resembled those reported previously for copper-containing Nir of other bacterial systems. The peculiar features of the Nir Type 1 center—its blue-green color with absorbance at 457 nm at least as large as that at 589 nm, its rhombic EPR spectrum, and its ~250-mV reduction potential—were consistent with properties of previously reported Nir. Sufficient amounts of the present enzyme were available to estimate that the midpoint potential of the nitrite-free Type 2 center was below 200 mV (Figure 6). If the WT Type 1 center with a midpoint potential of 247 mV is to perform as an effective internal electron donor in Nir, the reduction potential of the Type 2 center must increase above 200 mV when nitrite binds to the Type 2 cupric center (*6*). The sharpening and change of Type 2 EPR features (Figure 2B) in the presence of nitrite provided us an impetus for studying the underlying electronic structural reasons by ENDOR of Type 2 histidine nitrogen and proton features and for discovering an electronic structural decrease in covalent ligand spin density brought on by nitrite binding. This discovery may be consistent with an increase of the midpoint potential of the Type 2 center (next paper).

M182T. The results of this single-point mutation shed light both on intrinsic properties of a Type 1 center and on the Type 1 function within Nir. Changing Met to Thr would diminish the strength of the Type 1 axial ligation. The effect of this change was to cause an obvious color shift from a blue-green to a blue Type 1 protein, as shown in Figure 1. The mutation of the methionine ligand to threonine evidently

destabilized the cupric state (or stabilized the cuprous state) and thereby raised the Type 1 reduction potential so that the reduction potential of the blue M182T mutant then became similar to that of the blue protein plastocyanin which has a potential $E° = 370$ mV (*15*). A detailed experimental and theoretical explanation provided in ref 12 for the difference between a Type 1 blue center of plastocyanin and the Type 1 blue-green center of Nir is that the unusually short Met(S)−Cu bond in blue-green Nir leads to a distortion of the Type 1 liganding environment. This distortion causes associated optical changes and changes in the ground state HOMO (highest occupied molecular orbital) wave function that contains unpaired electron spin. We find that the change in optical and redox properties is indeed coupled to change brought on by the single M → T point mutation of the axial ligand. The electronic properties of the M182T cupric ground state (*g* values and copper hyperfine values here, ENDOR-determined spin densities at histidine and cysteine in the next paper) were unchanged from their values in the wild-type blue-green Type 1 center. We infer from the comparison of our WT Nir, M182T, and plastocyanin that the Met(S) ligation is a determinant of optical and possibly redox changes. However, the cupric ground-state electronic structure reflects the status of the Type 1 histidine and cysteine ligands, as they respond to more complex differences in protein conformation between Nir (both WT and M182T) and plastocyanin. These conformational differences may transcend a simple liganding change and involve perturbing H-bonds, tertiary interactions, and strains whose effects are relayed to the Type 1 copper by its histidine and cysteine ligands. [See Figure 1 of Adman (*37*) for a pictorial compendium of protein factors which may affect Type 1 copper site properties.] M182T had an activity that was no more than an order of magnitude smaller than that of the WT enzyme. The mutation-induced increase in midpoint potential for the Type 1 center of M182T and the resultant decreased driving force for electron transfer to the Type 2 center would provide an explanation for the decreased activity of the M182T mutant, although the Met^{182} ligand is not in the obvious electron-transfer pathway either to the Type 2 center, or before that, from the reductant binding patch (*6*).[8] The blue Type 1 center of M182T with its 354-mV midpoint potential still functions to shuttle electrons to the Type 2 center in the presence of nitrite. A blue-green center is not essential to Nir enzyme activity, as shown by the fact that Nir of *Alcaligenes xylosoxidans* (*38*) has a blue Type 1 center.

H287E. The H287E mutation near the Type 2 center markedly altered activity but not as a mutation that simply eliminated the Type 2 center. The histidine and water proton ENDOR features of the Type 2 center of H287E continued to resemble those of WT enzyme (next paper). Rather, judged from the ∼4-Å proximity of the nonliganding N_δ of His^{287} to the Type 2 copper and the proximity of His^{287} to the axial ligation site (*6*), the mutation must have perturbed nitrite binding and/or water release. A simple explanation is that the negatively charged carboxylate of the glutamate repels the nitrite ligand so that water does not leave. Consistent with its 100-fold slower activity than the WT enzyme, the H287E mutant did not spectroscopically respond to nitrite, insofar as it showed no EPR change in the presence of nitrite (Figure 2C′ vs 2C″).

Implications for the Reaction Mechanism. Experiments with WT Nir suggest that in the presence of biologically relevant cytochrome or pseudoazurin reductants ($E°$ ∼250 mV) and in the absence of nitrite, the Nir enzyme likely exists in a mixed-valence form where the Type 1 center ($E°$ ∼250 mV) is significantly reduced and the water-bound Type 2 center ($E°$ <200 mV) is oxidized. Our ENDOR spectroscopy study (next paper) shows that binding of nitrite to oxidized Type 2 copper has an obvious effect upon the electronic structure of the Type 2 center. We suggest that such binding of nitrite to the oxidized Type 2 center of the mixed-valence enzyme is the trigger that raises the Type 2 reduction potential and induces catalytic electron transfer. This model is supported by the observation that M182T still has considerable activity, and the M182T mutant with its ∼100 mV higher Type 1 potential is even more likely to be in a mixed-valence state in the absence of nitrite than the WT enzyme. It is difficult to understand how the Type 2 center in this mutant would be reduced by the Type 1 center before nitrite binds, as required by other models of Nir activity (*19*). Nitrite binding to the Type 2 center requires not only copper but also an optimal arrangement of charge and hydrogen-bonding environments around the center. The marked loss of activity due to H287E showed that changes in the Type 2 center beyond its immediate copper ligands can have a critical impact on activity, and ENDOR experiments (next paper) show why. To probe rapid redox and catalytic interaction, limited turnover stopped-flow and freeze-quench experiments on the copper centers are underway.

ACKNOWLEDGMENT

Prof. R. P. Cunningham, SUNY Albany Department of Biological Sciences, kindly provided FPLC purification of enzymes via Q-sepharose ion-exchange chromatography and gel-filtration chromatography. We would like to thank Adam Borah, Joe Shipman, and Wei-Li Lu for help in the early stage of this project.

SUPPORTING INFORMATION AVAILABLE

A detailed discussion of the development of the Nir−maltose binding fusion system, Figure S-1 showing optical spectra in the 350−900-nm range from TD-WT, TD-H287E, and TD-M182T, and Figure S-2 showing a double-reciprocal plot of Nir activity as it was followed by the rate of oxidation of cyt c^{2+} in the presence of varying amounts of nitrite (4 pages). Ordering information is given on any current masthead page.

REFERENCES

1. Van der Oost, J., de Boer, A. P. N., De Gier, J.-W. L., Zumft, W. G., Southamer, A. H., and van Spanning, R. J. M. (1994) *FEMS Microbiol. Lett. 121*, 1−9.
2. Tosques, I. E., Kwiatkowski, A. V., Shi, J., and Shapleigh, J. P. (1997) *J. Bacteriol. 179*, 1090−1095.
3. Kwiatkowski, A. V., and Shapleigh, J. P. (1996) *J. Biol. Chem. 271*, 24382−24388.

[8] Even though we kept the same total copper in our activity measurements, it is conceivable that there are statistically more open copper sites in the M182T mutant that lead to less activity.

4. Schmidt, H. H. H. W., and Walter, U. (1994) *Cell 78*, 919−925.
5. Godden, J. W., Turley, S., Teller, D. C., Adman, E. T., Liu, M. Y., Payne, W. J., and LeGall, J. (1991) *Science 253*, 438−442.
6. Adman, E. T., Godden, J. W., and Turley, S. (1995) *J. Biol. Chem. 270*, 27458−27474.
7. Colman, P. M., Freeman, H. C., Guss, J. M., Murata, M., Norris, V. A., Ramshaw, J. A. M., and Venkatappa. (1978) *Nature 272*, 319−324.
8. Adman, E. T., Stenkamp, R. E., Sieker, L. C., and Jensen, L. H. (1978) *J. Mol. Biol. 123*, 35−47.
9. Iwasaki, H., Noji, S., and Shidara, S. (1975) *J. Biochem. (Tokyo) 78*, 355−361.
10. Michalski, W. P., and Nicholas, D. J. D. (1985) *Biochim. Biophys. Acta 828*, 130−137.
11. Kakutani, T., Watanabe, H., Arima, K., and Beppu, T. (1981) *J. Biochem. (Tokyo) 89*, 453−461.
12. LaCroix, L. B., Shadle, S. E., Wang, Y., Averill, B. A., Hedman, B., Hodgson, K. O., and Solomon, E. I. (1996) *J. Am. Chem. Soc. 118*, 7755−7768.
13. Reinhammar, B. R. M. (1972) *Biochim. Biophys. Acta 275*, 245−259.
14. Ainscough, E. W., Bingham, A. G., Brodie, A. M., Ellis, W. R., Gray, H. B., Loehr, T. M., Plowman, J. E., Norris, G. E., and Baker, E. N. (1987) *Biochemistry 26*, 71−82.
15. Sykes, A. G. (1991) *Struct. Bonding 75*, 175−224.
16. Ingledew, W. J., and Cobley, J. G. (1980) *Biochim. Biophys. Acta 590*, 141−158.
17. Suzuki, S., Kohzuma, T., Deligeer, Yamaguchi, K., Nakamura, N., Shidara, S., Kobayashi, K., and Tagawa, S. (1994) *J. Am. Chem. Soc. 116*, 11145−11146.
18. Kukimoto, M., Nishiyama, M., Murphy, M. E. P., Turley, S., Adman, E. T., Horinouchi, S., and Beppu, T. (1994) *Biochemistry 33*, 5246−5252.
19. Averill, B. A. (1996) *Chem. Rev. 96*, 2951−2964.
20. Maniatis, T., Fritsch, E. F., and Sambrook, J. (1982) *Molecular Cloning: A Laboratory Manual*, Cold Spring Harbor Press, Cold Spring Harbor, NY.
21. Hanna, P. M., Tamilarasan, R., and McMillin, D. R. (1988) *Biochem. J. 256*, 1001−1004.
22. Berks, B. C., Ferguson, S. J., Moir, J. W. B., and Richardson, D. J. (1995) *Biochim. Biophys. Acta 1232*, 97−173.
23. Hulse, C. L., Tiedje, J. M., and Averill, B. A. (1988) *Anal. Biochem. 172*, 420−426.
24. Wikström, M., Krab, K., and Saraste, M. (1981) *Cytochrome Oxidase, A Synthesis*, p 138, Academic Press, Inc., London.
25. Libby, E., and Averill, B. A. (1992) *Biochem. Biophys. Res. Commun. 187*, 1529−1535.
26. Jensen, P., Aasa, R., and Malmström, B., G. (1981) *FEBS Lett. 125*, 161−164.
27. Aasa, R., and Vänngård, T. (1975) *J. Magn. Reson. 19*, 308−315.
28. Bradford, M. M. (1972) *Anal. Biochem. 72*, 248−254.
29. Karlsson, B. G., Nordling, M., Pascher, T., Tsai, L., Sjölin, L., and Lundberg, L. G. (1991) *Protein Eng. 4*, 343−349.
30. Gewirth, A. A., and Solomon, E. I. (1988) *J. Am. Chem. Soc. 110*, 3811−3819.
31. Lu, Y., LaCroix, L. B., Lowery, M. D., Solomon, E. I., Bender, C. J., Peisach, J., Roe, J. A., Gralla, E. B., and Valentine, J. S. (1993) *J. Am. Chem. Soc. 115*, 5907−5918.
32. Gill, S. C., and von Hippel, P. H. (1989) *Anal. Biochem. 182*, 319−326.
33. Howes, B. D., Abraham, Z. H. L., Lowe, D. J., Brüser, T., Eady, R. R., and Smith, B. E. (1994) *Biochemistry 33*, 3171−3177.
34. Murphy, L. M., Strange, R. W., Karlsson, B. G., Lundberg, L. G., Pascher, T., Reinhammar, B., and Hasnain, S. S. (1993) *Biochemistry 32*, 1965−1975.
35. Solomon, E. I., Baldwin, M. J., and Lowery, M. D. (1992) *Chem. Rev. 92*, 521−542.
36. Wu, Q., Storrier, G. D., Pariente, F., Wang, Y., Shapleigh, J. P., and Abruña, H. D. (1997) *Anal. Chem.*, in press.
37. Adman, E. T. (1991) in *Advances in Protein Chemistry* (Anfinsen, C. B., Richards, F. M., Edsall, J. T., and Eisenberg, D. S., Eds.) Vol. 42, pp 145−197, Academic Press, San Diego.
38. Abraham, Z. H. L., Lowe, D. J., and Smith, B. E. (1993) *Biochem. J. 295*, 587−593.

BI971603Z